# Characterization of Focused Ultrasound induced Acoustic Streaming

**R. BEN HAJ SLAMA[a,b] ,B. GILLES[a], M. BEN CHIEKH[b] , J .C. BERA[a]**
a. Univ Lyon, Université Claude Bernard Lyon 1, INSERM, LabTAU UMR1032, F-69003, LYON, France
b. Université de Monastir, ENIM, LESTE, Monastir, Tunisie
rafika.ben-haj-slama@inserm.fr

## Abstract:

*This study is interested in one of the hydrodynamic mechanisms induced by High Intensity Focused Ultrasound (HIFU) propagation in a liquid medium, the acoustic streaming phenomenon. The latter is a flow generation caused by acoustic energy viscous dissipation during acoustic wave propagation in a fluid medium. Particle Image Velocimetry (PIV) technique was used to determine velocity fields in an infinite aquatic medium subjected to a focused ultrasonic field. These tests were carried out with a parametric variation, namely, of the applied acoustic pressure at the focus (ranging from 2 to 18.4 bars) and of the transducer frequency (550 kHz and 1 MHz). The experimental results allowed to characterize the mean streaming flow and in particular to evaluate the maximum axial velocity magnitude reached in the focal zone and conclude how the velocity increases with ultrasound wave amplitude and frequency.*

**Key Words: Focused ultrasound, Acoustic streaming, PIV, like-Jet flow**

## 1 Introduction

Acoustic streaming, which is the flow generated by the propagation of an ultrasonic wave in a fluid medium, is exploited in several applications. Nowadays, several studies suggest its use for optimizing crystallogenesis process and ensuring the crystalline material homogeneity by controlling temperature fluctuations [1,2]. This phenomenon is also an interesting way to improve heat dissipation of micro-devices such as micromechanical components [3]. For therapeutic applications, acoustic streaming is an important contributor in the sonothrombolysis technique which could treat certain cardiovascular diseases by destroying blood clots blocking blood circulation [4]. In this technique, acoustic streaming improves mixing in the treatment zone and thus makes thrombolytic agents more effective [6]. Acoustic streaming phenomenon has been known since the 1830s [7] and has since been the subject of several fundamental and experimental researches. However, few studies numerically [8,9] and experimentally [10,11,12] investigate acoustic streaming in the special case of focused ultrasound. Therefore, it is interesting to establish and append to these studies an experimental database explaining this hydroacoustic aspect.

If the longitudinal scale of the ultrasound wave propagation medium is much greater than the wavelength, a propagating wave is reported. Under these conditions, a steady flow appears in the liquid arising from the ultrasound absorption. This is called the Eckart streaming [13] where it is considered that the induced velocity is proportional to the square of the acoustic pressure. Later, Lighthill [14] established that this steady streaming motion is due to the Reynolds stress created by the viscous dissipation of the acoustic energy per unit volume, and added the hydrodynamic non linearity term in the Navier-Stocks equations. Lighthill reported that neglecting the nonlinearity effect is pertinent for week Reynolds number flows (Re<<1). Besides, in the case where the acoustic beam does not interact with the lateral walls of the domain, no acoustic boundary layer is present in the problem and Rayleigh streaming [15] is negligible compared to the Eckart streaming which will be the subject of this work.

Our analysis is limited to an incompressible and Newtonian fluid, and to the steady state of the streaming flow in the presence of acoustic stress, where the streaming motion definition is based on the Reynolds decomposition [14,16].

In this study, Particle Image Velocimetry (PIV) technique was used to investigate velocity fields in free liquid medium subjected to focused ultrasound field. Tests are carried out with a parametric variation, namely, of the applied acoustic pressure at the focus and of the wave frequency (maximum pressure magnitude $P_{ac}$ from 2.6 to 18.4 bar for $f$=550 KHz and from 2 to 10.5 bar for $f$=1 MHz).

# 2 Experimental procedure and methods

Experiments were carried out in a 60-l tank, filled with degassed and filtered water (rate of dissolved oxygen<2mg.l$^{-1}$). The tank walls were made of glass to allow optic access and water was seeded with spherical Polyamide Seeding Particles PSP (Dantec Dynamics) whose diameter is of 5 µm and density, close to that of water, of 1030 kg.m$^{-3}$ [17]. These seeding particles are shown to be reliable and appropriate to characterize the streaming flow under the experimental conditions of the study and to not undergo acoustic radiation pressure [18]. To generate the ultrasonic waves, tow piezoelectric focused transducers (with a 10 cm diameter and a 10 cm and 8 cm focal length) were used. The transducer was immersed 10 cm deep into the water tank and was fed at its resonance frequency (550 kHz and 1 MHz). The driving signal of the transducer was induced by a generator (Tektronix AFG3102, 100 MHz) which supplies an input voltage amplitude from 25 to 275 mV in continuous mode to a power amplifier (Prâna DP300, 53 dB gain), generating a maximum acoustic pressure amplitude at the focus, respectively, of 2 to 18.3 bar depending on the transducer used. An ultrasound absorber was placed at the end of the tank in front of the source in order to avoid standing wave generation. Velocity measurements were performed using the PIV technique. The PIV system used a laser source (Changchun New Industries Optoelectronics MGL-F-532-2W) with a wavelength of 532 nm, operating in continuous mode and generating a 2mm-diameter light beam. The laser beam was converted, using an optical system consisting of a lens assembly, to a 20cm-wide and 250µm-thick laser sheet, and then positioned to illuminate the measuring area including the focal zone. Due to the light scattered by the seeding particles, particle flow was recorded by a CMOS-based camera (Vision Research Phantom V12.1). 1280 x 800 pixel resolution images were acquired at a rate of 24 frames per second with an exposure time of 41.7ms. The resulting field of view dimensions were 9cm x 5.6cm. The experimental set up is illustrated in Figure 1.

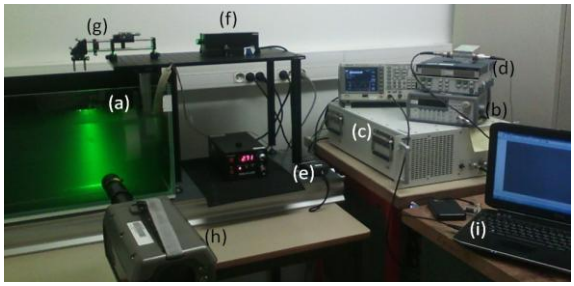


Figure 1 : Experimental setup: {Acoustic streaming generation system: (a) Ultrasound transducer immerged in a 60 l water tank, (b) voltage generator, (c) amplifier, (d) wattmeter, (e) thermocouple}, {PIV measurement system: (f) Laser, (g) optical assembly, (h) CMOS camera, (i) data storage}.

To solve the seeding particle velocity field, each pair of images was cross-correlated using PIVlab (a set of routines built in MATLAB [19]) and adopting an algorithm using Fast Fourier Transform (FFT). This algorithm is adaptive and based on an initial assessment of velocity vectors on large interrogation windows (128 pixels x 128 pixels). Interrogation area size is gradually reduced to reach ultimately a size of 32x32 pixels (about 2.2 by 2.2 mm). This final interrogation window size is the optimal one and has been selected for image processing after velocity convergence test depending on the size of the final interrogation window. It is generally convenient that the interrogation window comprises more than 5 particle images [20] and this condition was fulfilled with the introduced particles quantity mentioned above. Frame time step was also tested to carry out correlation with an optimal one that takes into account the velocity scales. This convergence test led us to choose a 83.3 ms time step between 2 images, which is two times the original recording time step (41.7 ms).
To get a stable and properly averaged field, we have shown in a previous study [18] that a number of 50 image-pairs was sufficient for the averaging and waiting 60s before recording the images was enough to reach the stability. In the present study, a number of 200 image-pair has been chosen for averaging to make sure of the stability of the streaming flow in the highest applied acoustic pressure.

# 3 Results

## 3.1 Time-averaged flow field

A preliminary view of the HIFU influence on the stagnant water is provided by the time-averaged flow field. The distributions of the axial velocity component for different acoustic pressures are shown in Figure 2. Axial velocity distributions highlight the development of a local area of increased velocity magnitude around the HIFU focus location with a peak in the near region of this focus witch correspond to the acoustic streaming. For all cases, axial velocity had roughly a symmetric distribution with respect to the y-direction. The affected area grows in size with the acoustic pressure increase with a significant spreading in the x-direction.
The induced flow seemed to be greatly affected by the excitation parameters: pressure and frequency. An important variation of the velocity magnitude is noticed. For both studied frequencies, when the acoustic pressure increased, centerline maximum velocity value is continuously shifted towards large values x coordinate. A maximum value of 3.1 cm/s is reached at the limit of the operating condition (at $f$=1 MHz and $P_{ac}$=10.5 bar).

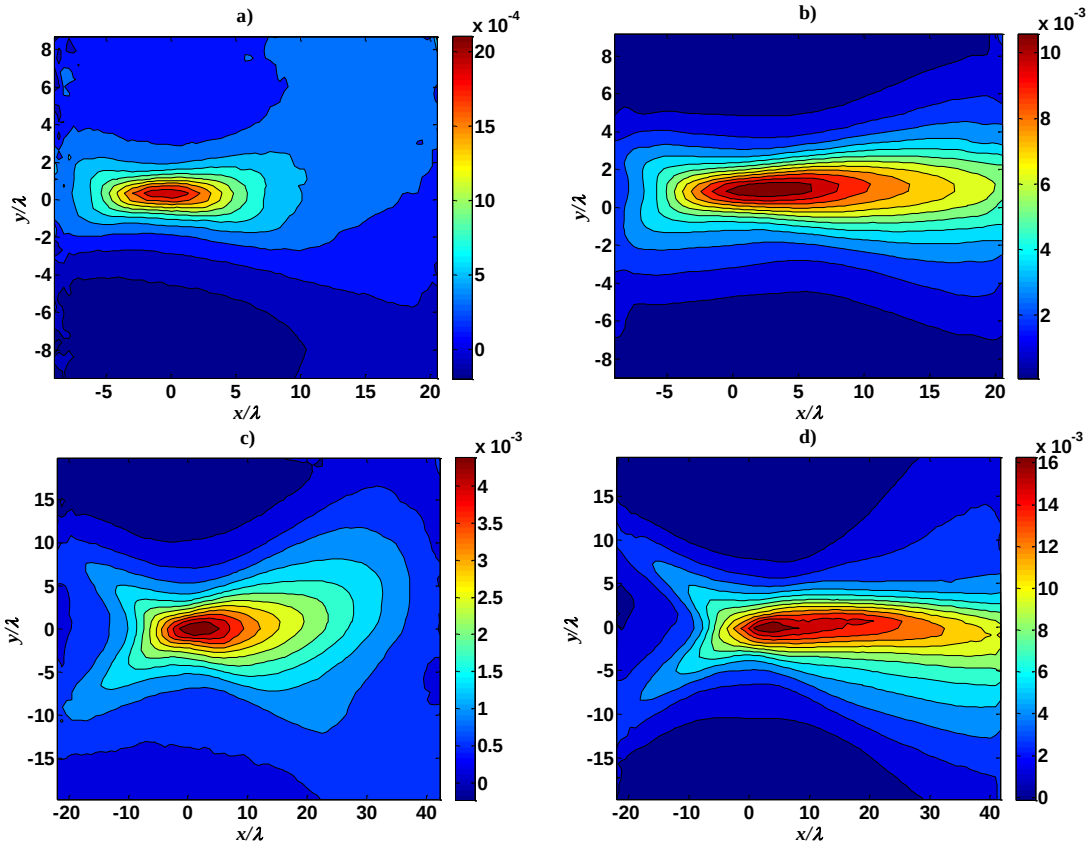


Figure 2: Distribution of axial velocity in the measurement plane ($x/\lambda$, $y/\lambda$) at $f$=550 kHz for different applied acoustic pressure a) $P_{ac}$ =5.2 bar and b) $P_{ac}$ =15.7 bar and at $f$=1 MHz for different applied acoustic pressure c) $P_{ac}$=2 bar and b) $P_{ac}$=6 bar. Transducer focus position = (0,0), Ultrasound waves are coming from the left side.

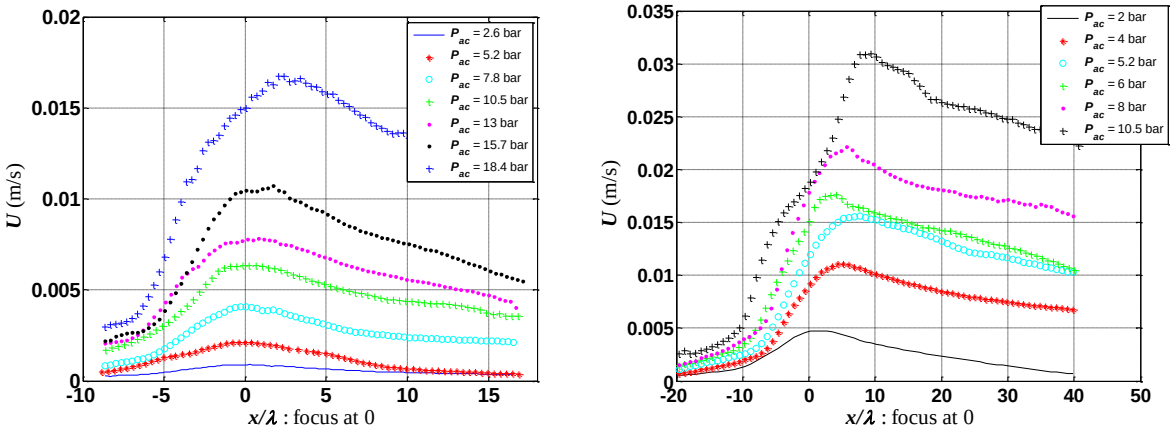


Figure 3: Axial velocity magnitude throughout the focal axis. Right ($f$=550 kHz), left ($f$=1 MHz). Geometric focus at $x$=0

These results are shown for a larger pressure range in Figure 3, where we only show the velocity amplitude evolution along the acoustic axis depending on different applied maximum pressures and on the two wave frequencies. From these Figures, we can notice that when doubling the frequency, the velocity amplitude raises with a rate of about 5.5 times for an applied pressure less than 10.5 bar. Beyond this pressure, velocity increases of about 6 times. We can also notice that both longitudinal expansion of the streaming field downstream of the focus and maximum velocity position shift regarding the focus, increase with the pressure for both frequencies.

Plots of the maximum values of the centerline velocity at different acoustic pressure for both studied frequencies are shown in Figure 4. For f=550 kHz, this maximum increased at roughly constant rate up to $P_{ac}$=15.7 bar and the evolution may be assumed to be linear before switching to another kind of variation. For $f$=1 MHz, the linear variation is observed for the entire range of the operating acoustic pressure, but with a more important slope when compared to the previous frequency.
In the following sections, results presentation and their discussions are limited to two selected acoustic pressure for each studied frequency within the linear regime mentioned above. The chosen pressure values are $P_{ac}$=5.2 and 15.7 bar for the first studied frequency $f$=550 kHz and $P_{ac}$ =2 and 6 bar for the second studied frequency $f$=1MHz.

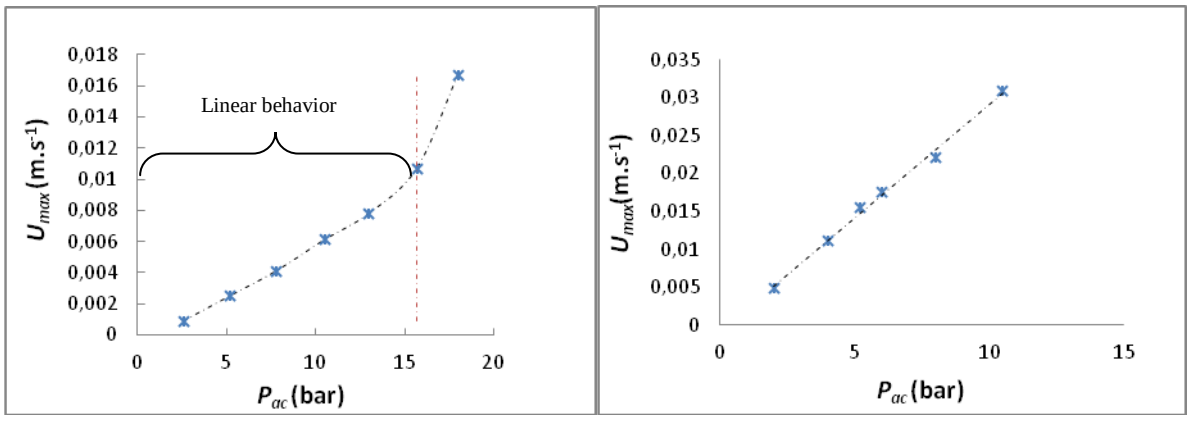


Figure 4: Maximum axial velocity evolution versus the acoustic pressure amplitude. Left: $f$= 550 kHz, right: $f$=1MHz

This linear behavior can be explained by a scaling analysis of the streaming force. In the case of a planar ultrasound transducer reported by Moudjed et al. [21] such a scaling was based on a threshold axial position depending on Fresnel distance and wave diffraction laws. According to this scaling the streaming field was divided in two regions with respect to the threshold position $x_{lim}$: a near field starting from the ultrasound source (the transducer surface) up to $x_{lim}$, where the inertial force has the dominant role in the streaming motion and this scaling law leads to a velocity-pressure linear relation, and a far field ($x$> $x_{lim}$) where the viscous force plays a dominant role in the forces balance and a quadratic law relates the streaming velocity to the acoustic pressure.
In the present work we are studying a focused ultrasound transducer and the jet source does not extend from the transducer surface up to very far but is limited to the focal zone. Thus, our study concentrates on the focal zone where the streaming flow is accelerated and inertial term is dominant against the viscous term.
We give the following brief reasoning in the axial scale, with referring to the balance force equation below where drag and gravity forces are neglected:

$$\rho \frac{\mathrm{d}u}{\mathrm{d}t} = \beta p_{ac}^2(x) \tag{1}$$

Where $p_{ac}$ is the acoustic pressure amplitude at the position $x$, $\rho$ is the fluid density and $\beta$ is a coefficient depending on the attenuation coefficient and the sound speed in the liquid. Considering the steady state, we obtain:

$$\rho \frac{\partial}{\partial x}\left(\frac{u^2}{2}\right) = \beta \, \mathrm{p}^2(x) \tag{2}$$

Integrating along the accelerated part of the trajectory provides:

$$u_{\max}^2 = 2\frac{\beta}{\rho}\int_0^L p_{ac}^2(x)dx \quad (3)$$

If the position of the maximum velocity is fix (case of f=550 kHz, except the last point Pac = 18.4 bar) one directly obtains that the maximum velocity is proportional to the maximum pressure amplitude at the focus ($x$=0).

$u_{max} \propto P_{ac} = p_{ac}(x=0)$ (4)

In a previous study [18], the streaming flow was proven to be stable for the pressure range below 15.7 bar and a laminar regime was adopted in numerical simulations providing results in good agreement with the experimental ones, so that we can confirm that cavitation does not occur below this pressure amplitude. Regarding the particular case of ($P_{ac}$ = 18.4 bar, $f$= 550kHz) where pressure-velocity dependence is not linear; low cavitation appearance can be the cause behind.

## 3.2 Jet-like behavior of the streaming

This part of the study was inspired from previous investigations namely those of Moudjed et al. [21] and Dentry et al. [22] where the streaming generated by a planar ultrasound beam was considered as a free jet flow. In order to hydro-dynamically characterize the streaming flow, cross stream variations of the mean axial velocity are plotted for selected pressure and frequencies in Figure 5. The profiles show the existence of a non-zero –velocity region on either side of the focus $x$=0 with large values downstream the focus as seen in figure 2. Velocity profiles display the traditional jet-like profiles that spread laterally with increasing $x/\lambda$. All profiles are symmetric with respect to the y-axis. The lateral spreading extend until large values of $x/\lambda$ which leads to uniform profile accompanied with a decay of the mean centerline velocity as shown in the transverse profile $x/\lambda$=30 for $P_{ac}$ =2 bar and $f$=1MHz.

As shown in Figure 6. Profiles evolution may be subdivided in two regimes: a rapid rising rate upstream the maximum location over a distance in the range of 10 to 15 $\lambda$ and a slow decay phase downstream. In the second regime, a near self-similar state evolution of the mean axial velocity may be obtained when plotted normalized by the local centerline velocity $U_c$ versus shifted origin location from HIFU focus location to the maxima location of the velocity profiles.

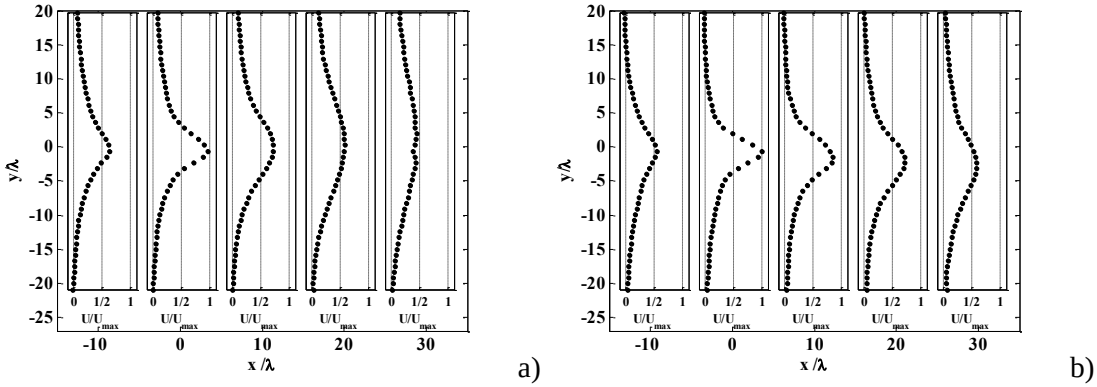


a) b)

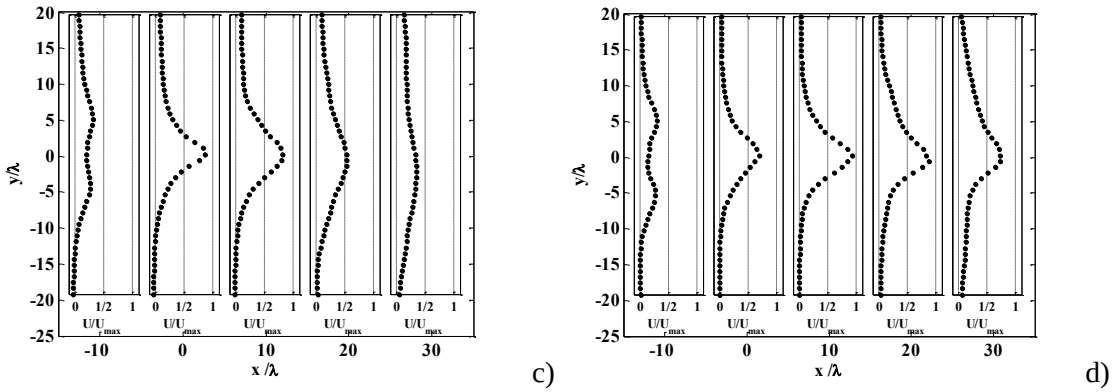


Figure 5: Streamwise and transverse variations of the mean axial velocity at *f*=550khz for different applied acoustic pressure a) $P_{ac}$ =5.2 bar and b) $P_{ac}$ =15.7 bar and at *f*=1 Mhz for different applied acoustic pressure c) $P_{ac}$ =2 bar and b) $P_{ac}$ =6 bar.

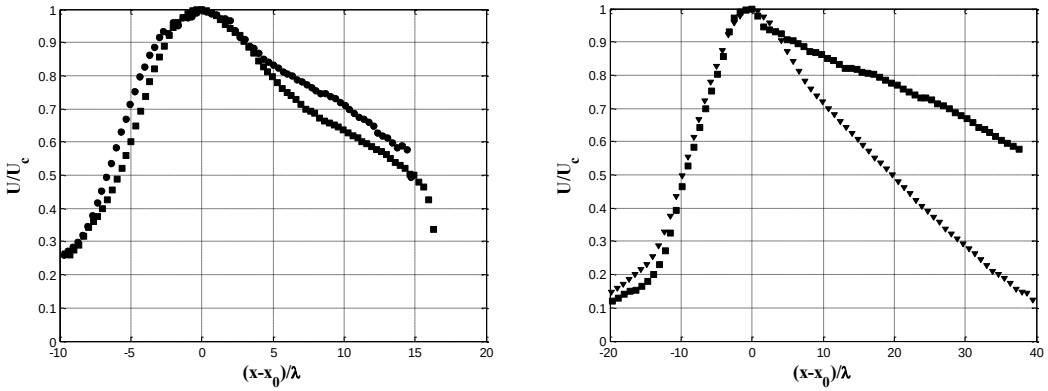


Figure 6: Mean axial velocity profiles at the axis *y*=0 normalized by the centerline velocity $U_c$ (left) at *f*=550 kHz for different applied acoustic pressures $P_{ac}$ =5.2 bar (■) and b) $P_{ac}$ =15.7 bar (●)and (right) at *f*=1 Mhz for different applied acoustic pressure $P_{ac}$ =2 bar (▼) and b) $P_{ac}$ =6 bar (◀). The x-axis was shifted by the maxima locations

To further characterize the like-jet behavior observed for the streaming flow, Figure 7 showed the cross flow profiles of the streamwise velocity normalized by the local maxima $U_c$. The profiles nearly collapse except at large *y* values where velocity measurements are more prone to errors, indicating that the near focus region flow reached a self-preserved stat. The lateral flow spreading is accompanied with a decay of the mean centerline velocity and an expansion of the jet-like flow width whereby momentum remains constant.

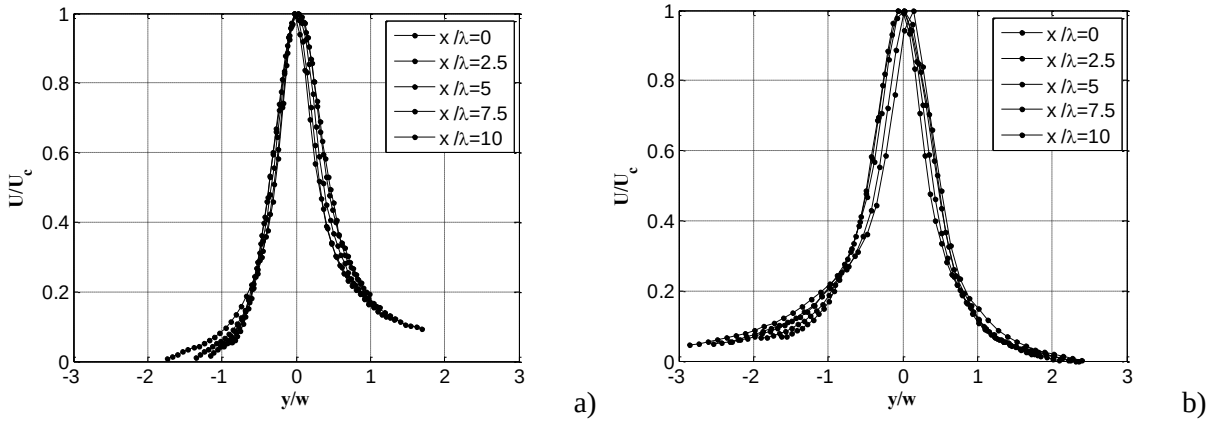


Figure 7 : Streamwise and transverse variations of the mean axial velocity normalized by the local maxima $U_c$ at different locations downstream the maxim location for a) $P_{ac}$=5.2 bar b) $P_{ac}$ =15.7 bar. *f*=550 kHz

For the streaming, self-similar state is clearly observed downstream of the maximum location. It is necessary to recall here that for a traditional jet flow, the self-similarity state is reached at about $x=4D$ to $6D$ where $D$ is the hydraulic diameter of the nozzle.
The jet-like flow width $w$, estimated as the distance between the locations of the 50% $U_c$, is shown in Figure 8. The data suggests that the flow width is roughly constant upstream the maximum location and grows linearly with the downstream distance from the maximum location and for the range of $x/\lambda$ reported here, the jet width increased roughly at a constant rate of 0.5 for lower acoustic pressure and 0.2 for high acoustic pressure.

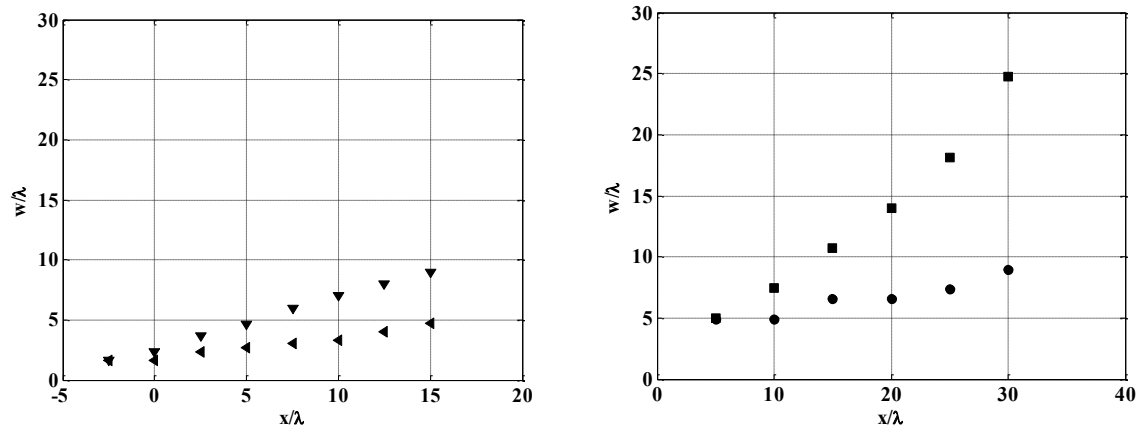


Figure 8: Streaming width evolution. (left) at $f$=550 kHz for tow applied acoustic pressures: $P_{ac}$ =5.2 bar (▼) and $P_{ac}$ =15.7 bar (◀).(right) at $f$=1 Mhz for tow applied acoustic pressures: $P_{ac}$ =2 bar (■) and $P_{ac}$ =6 bar (●). The $x$-axis was shifted by the maxima locations

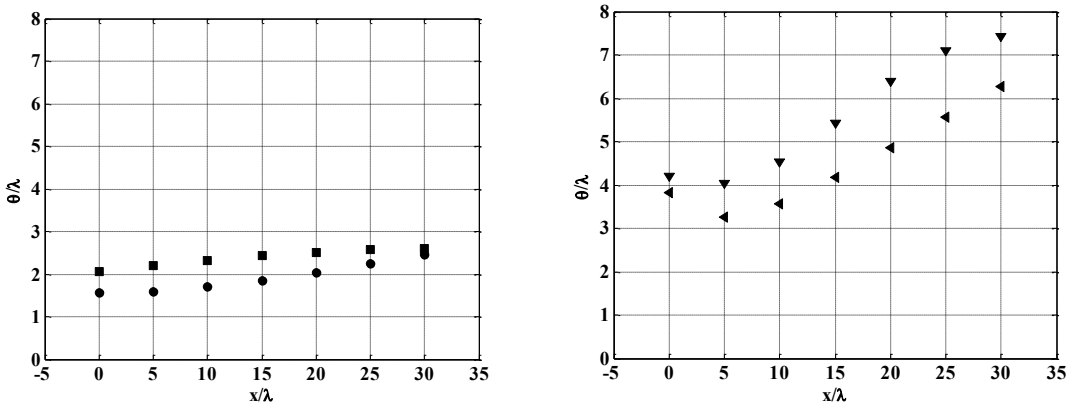


Figure 9 : Streaming momentum thickness evolution (left) at $f$=550 kHz for different applied acoustic pressures $P_{ac}$ =5.2 bar (■) and b) $P_{ac}$ =15.7 bar (●)and (right) at $f$=1 MHz for different applied acoustic pressure $P_{ac}$ =2 bar (▼) and b) $P_{ac}$ =6 bar (▶). The $x$-axis was shifted by the maxima locations

The momentum thickness associated to the streaming flow is evaluated as:

$$\theta = \int_{y_{\min}}^{y_{\max}} \frac{U(y)}{U_{\max}}\left(1-\frac{U(y)}{U_{\max}}\right)dy$$

and is illustrated in Figure 9.

The momentum increases slightly upstream the maximum velocity location but increased at much faster rate downstream. Its values upstream the maximum location is in the range of 3 to 5 $\lambda$. $\theta$ increases with downstream distances at a rate of about 0.1. It can be, also, noticed that the momentum thickness grows inversely with the applied acoustic pressure for the two applied frequencies.

# Conclusions

This study concerns the experimental characterization of the acoustic streaming and fluid dynamic behavior induced by focused ultrasound propagation in liquid medium. Experiments were carried out using Particle Image Velocimetry technique. Experimental tests were conducted with a parametric variation of the wave frequency (0.55 and 1MHz) and of the applied acoustic pressure (from 2 to 18 bar at the focus). The study investigates a large range of acoustic pressure amplitude where streaming velocity grows linearly with this amplitude (below 15.7 bar at the focus). Results show that the streaming flow generated by focused ultrasound field presents interesting similarities compared to a classical free jet flow.

# Acknowledgments

This work which is conducted within a joint thesis supervision between the LESTE laboratory (Laboratoire des Systems Thermiques et Energétiques) of the National School of Engineers of Monastir-Tunisia and the LabTAU laboratory (Laboratoire des Applications des Ultrasons à la Thérapie) of the National Institute of Health and Medical Research Lyon-France, was supported by the French National Research Agency (LabEx CelyA ANR-10-LABX-0060/ANR-11-IDEX-0007, Project "ULysSE" ANR- 11-JSV5-0008) and by Campus France (Hubert Curien Partnership PHC Utique 2017, 34886WB-STIC)

# References

[1] Dridi W, Henry D and Ben Hadid H (2007) Influence of Acoustic Streaming on the Stability of an Isothermal or Laterally Heated Fluid Layer, *C. R. Mecanique* 335

[2] Dridi W, Henry D and Ben Hadid H (2010) Stability of Buoyant Convection in a Layer Submitted to Acoustic Streaming, *Phys. Rev*, E81, 056309

[3] Wan Q, Wu T, Chastain J, Roberts W L, Kuznetsov A V, Ro P I (2005) Forced Convective Cooling via Acoustic Streaming in a Narrow Channel Established by a Vibrating Piezoelectric Bimorph, *Flow, Turbulence and Combustion*, Vol. 74, pp 195-206

[4] Siegel R J, Luo H (2008) Ultrasound Thrombolysis. *Ultrasonics*, vol.48, pp 312-320

[5] Rosenschein U, Furman V, Kerner E, Fabian I, Bernheim J, Eshel Y (2000) Ultrasound Imaging-Guided Noninvasive Ultrasound Thrombolysis: Preclinical Results. *Circulation*, vol.102, pp 238-245

[6] Sakharov D V, Hekkenberg R T and Rijken D C (2000) Acceleration of Fibrinolysis by High-frequency Ultrasound: the Contribution of Acoustic Streaming and Temperature Rise, *Thromb. Res*, Vol.100, pp 333-340

[7] Faraday M, Acoustic Streaming, *Phil. Trans*., vol.121, pp 229(1831).

[8] Wu J and Du G (1993) Acoustic Streaming Generated by Focused Gaussian Beam and Finite Amplitude Tonebursts, *Ultrasound in Med. & Bio.*, Vol 19. No 2, pp 167-176

[9] Kamakura T and Breazeale M A (1995) Acoustic Streaming Induced in Focused Gaussian Beams, *J. Acoust. Soci. Am.*, 97, 2740

[10] Nowicki A, Kowalewski T, Secomski W, Wojccik J (1998) Estimation of Acoustical Streaming: Theoretical Model, Doppler Measurements and Optical Visualization, *Eur. J. Ultrasound* 7 73–81,

[11] Hariharan P, Myers M R, Robinson R A, Maruvada S H, Silwa J, Banerjee R K (2008) Direct Characterization of High Intensity Focused Ultrasound Transducers using Acoustic Streaming, *J. Acoust. Soc. Am.*, 123,1706–1719

[12] Tan A C H and Hover F S, Correlating the Ultrasound Thrust Force with Acoustic Streaming velocity, Institute of Electrical and Electronics Engineering IEEE International (2009) 2627–2630.

[13] Eckart C, Vortices and Streams Caused by Sound Waves, *Phys. Rev*, vol. 73, pp 68-76(1948).

[14] Lighthill S J (1978) Acoustic Streaming, *J. Sound Vibration*, vol. 61, pp 391-418

[15] Rayleigh L (1884) On the Circulation of Air Observed in Kundt's Tube, and on Some Allied Acoustical Problems, *Philos. Trans. R. Soc. London*, vol. 175, pp 1-21

[16] Lighthill S J (1978) Waves in Fluids, *Cambridge Univ*

[17] DANTEC Dynamics, SAFEX® Fog Generator Systems, "Safe Seeding for Flow Visualisation and LDA Applications"

[18] Ben Haj Slama R, Gilles B, Ben Chiekh M, Béra J C (2017) PIV for the Characterization of Focused Field Induced Acoustic Streaming: Seeding Particle Choice Evaluation, *Ultrasonics*, Vol.76, pp 217-226

[19] Thielicke W and Stamhuis E J (2014) PIVlab – Time-Resolved Digital Particle Image Velocimetry Tool for MATLAB (version 1.4)

[20] Keane R D and Adrian R J (1992) Theory of Cross-correlation Analysis of PIV Images, *Appl. Sci. Res.*, vol.49, pp 191-215

[21] Moudjed B, Botton V, Henry D, Ben Hadid H, Garandet J P (2014) Scaling and Dimensional Analysis of Acoustic Streaming Jet, *Phys. Fluids* 26 093602.

[22] Dentry M B, Yeo L Y, Friend J R (2014) Frequency Effects on the Scale and Behavior of Acoustic Streaming, *Phys. Rev*. 89 013203.